Astrophysics and Space Science (2006) 301:21–31
DOI 10.1007/s10509-006-5249-1

ORIGINAL ARTICLE

Scattering Properties and Composition of Cometary Dust

Ranjan Gupta · D.B. Vaidya · J.S. Bobbie · Petr Chylek

Received: 17 September 2003 / Accepted: 11 April 2005

Abstract Composition of the Comet dust obtained by the dust impact analyzer on the Halley probes indicated that the comet dust is a mixture of silicate and carbonaceous material. The collected interplanetary dust particles (IDP's) are fluffy and composite, having grains of several different types stuck together. Using discrete dipole approximation (DDA) we study the scattering properties of composite grains. In particular, we study the angular distribution of the scattered intensity and linear polarization of composite grains. We assume that the composite grains are made up of a host silicate sphere/spheroid with the inclusions of graphite. Results of our calculations on the composite grains show that the angle of maximum polarization shifts, and the degree of polarization varies with the volume fraction of the inclusions. We use these results on the composite grains to interpret the observed scattering in cometary dust.

Keywords Dust · Scattering · Comets · Polarization

R. Gupta (✉)
IUCAA, Ganeshkhind, Pune, India
e-mail: rag@iucaa.ernet.in

D.B. Vaidya
Gujarat College, Ahmedabad, India
e-mail: dbv@satyam.net.in

J.S. Bobbie
Institute for Atmospheric Science, University of Leeds, Leeds, UK

P. Chylek
Space and Remote Sensing Sciences, Los Alamos National Laboratory, Los Alamos, NM, USA

1. Introduction

In situ sampling of comet dust composition obtained by the dust impact analyzer on the Halley probes indicated a composition which is a mixture of silicate and carbonaceous material (Kissel et al., 1986; Jessberger et al., 1988; Jessberger, 1999). The collected interplanetary dust particles (IDPs) of likely cometary origin are fluffy and composite (Brownlee, 1987) and are typically of submicron to micron sized silicate grains embedded in a carbon rich matrix (Bradley et al., 1992). The laboratory studies of the composite particles (Chylek et al., 1988) and aggregates (Gustafson and Kolokolova, 1999) show that the scattering properties for these irregular and inhomogeneous particles are different from that of solid homogeneous particles. Mie theory for spherical particles is not capable of explaining the scattering properties of cometary dust particles because cometary particles are fluffy and nonspherical (see e.g. Jockers, 1997). Hence, there is a need to formulate models of electromagnetic scattering by the inhomogeneous and nonspherical grains. Calculations based on the discrete dipole approximation (DDA) (Purcell and Pennypacker, 1973; Draine, 1988; Lumme et al., 1997; Wolff et al., 1998) allow the study of the light scattering properties of the irregularly shaped and inhomogeneous grains. Xing and Hanner (1997) and Yanamandra-Fisher and Hanner (1999) have studied the scattering properties of the aggregates of silicates and carbonaceous material to interpret the observed polarization in comets. However, the shape of the polarization curve for the cometary dust is still not very well explained and also it is not very clear how the silicate and absorbing grains are mixed in the cometary dust (Hanner, 2002). Petrova et al. (2000) have shown that aggregates composed of touching spheres with size parameters 1.3–1.65 display properties typical of cometary particles; viz. a weak increase of the back scattering intensity, negative linear polarization at small phase angles ($\leq 20^{\circ}$) and a positive wavelength gradient polarization. Their results on the aggregates indicate that more compact particles have a more pronounced negative branch of polarization. Lamy et al. (1987) had suggested a composite grain model of silicate and graphite 'rough' grains to fit the observed polarization curve in the dust coma of comet Halley. The polarization of comet Halley was also observed at near IR wavelengths (viz. 1.25, 1.65 and 2.2 μm) at several phase angles by Brooke et al. (1987). They found that P/Halley exhibited a negative linear polarization branch at small phase angles i.e. $\leq 20^{\circ}$. They modeled their observations using solid Mie particles with two different compositions, one component being of very absorbing material. However they suggested a two component grain model with irregular grains for better understanding of the scattering properties of cometary dust. Jones and Gehrz (2000) have observed the polarization of dust in Comet Hale-Bopp in the K-band (2.2 μm) and they found the negative branch of polarization was much reduced (almost negligible) in the K band compared to that was observed in the visual wavelength range. Kelley et al. (2004) have observed several comets in the K-band (i.e. 2.2 μm) and have found that the K-band polarization was only 1–2% higher than typical optical polarization observed for the comets (Levasseur-Regourd et al., 1996). Kelley et al. (2004) also found that the comet Hale-Bopp showed no significant negative polarization branch at 2.2 μm at large scattering angles. For cometary dust the radiative energy received from Sun is either absorbed/and in part re-radiated in the thermal infrared wavelength range or is scattered. Harker et al. (2002) have used a fractal porous model of the amorphous carbon and amorphous silicate grains to model thermal emission from the dust coma of comet Hale-Bopp. In order to produce the fractal porous grain model, Harker et al. (2002) have used the effective medium approximation (EMA). However, it is to be noted that the EMA does not take into account the inhomogeneities within the structure or the surface roughness of the grains (see for example Wolff et al., 1998).

In the present study we are concerned with the scattered part of the solar radiation and it can be observed in the *uv*, visual and near infrared wavelength ranges upto about 3 μm; when the thermal radiation starts to become important (see for example Jockers, 1997).

In this paper we use the results of the DDA calculations on the composite grains with various mixing ratios of the constituent materials to explain the observed scattering properties, namely the angular distribution of the scattered intensity and linear polarization of cometary dust.

DDA has been used earlier by us to study the scattering properties of a composite particle made up of a host water sphere with carbon inclusions (Chylek et al., 2000). Recently we have used DDA to study the extinction properties of the composite grains (Vaidya et al., 2001). In the present study, we calculate the angular distribution of the scattered intensity and linear polarization for the spherical and non-spherical composite grains with silicate and graphite as constituent materials. The composite grains are assumed to be made of the host silicate sphere (or spheroid) with inclusions of graphite. We study the effect of the inclusion size and volume fraction on the angular distribution of the scattered intensity and the linear polarization for the composite grains. It is to be noted that the composite grain model we present here for cometary dust is different from the aggregate grain model of monomers suggested by Xing and Hanner (1997). In Section 2, we present the composite grain models. In Section 3 we give the results of our calculations and compare the results of the models ith the observations. Summary and conclusions are given in the last Section 4.

2. Discrete dipole approximation (DDA) and composite grain model

The basic DDA method consists of replacing a particle by an array of N oscillating polarizable point dipoles (see e.g. Draine, 1988). The dipoles are located on a lattice and polarizability is related to the complex refractive index m through a lattice dispersion relationship (Draine and Goodman, 1993). Each dipole responds to the external incident electric field and also to the electric fields of the other N-1 dipoles that comprise the particle. The polarization at each dipole site is therefore coupled to all other dipoles in the particle. There are two validity criteria for the DDA to provide accurate results (see e.g. Draine and Flatau, 1994; Wolff et al., 1994); viz (i) $|m|kd \leq 1$, where m is the complex refractive index, k is the wave number, $k = \pi/\lambda$ and d is the distance between the dipoles; and (ii) d should be small enough (N should be sufficiently large) to describe the shape of the particle satisfactorily. In the present study we use the modified DDA code (Dobbie, 1999; Vaidya et al., 2001) to calculate the angular distribution of the scattered intensity and the linear polarization P for a composite grain. The code, first carves out an outer sphere (or spheroid) from a lattice of dipole sites. Sites outside the sphere are vacuum and sites inside are assigned to be the host material. Once the host particle is formed the code locates centers for internal spheres to form the inclusions. The inclusions are of a single radius and their centers are chosen randomly. The code then outputs a three dimensional matrix specifying the material type at each dipole site which is then read by the DDA. In the present case, the sites are either silicates, graphites or vacuum. The porosity P of the composite grain is defined as the relative amount of volume filled by the vacuum in the composite grain and is given by $p = 1 - V_{\mathrm{solid}}/V_{\mathrm{total}}$, where

Table 1 Composite grain models

Shape of host grain	Number of dipoles, N	Volume fraction of inclusions, f	Size of inclusions, n
Sphere (Si+Gr)	57856	0.1	12
		0.2	12
		0.3	12
		0.2	6
		0.2	8
Spheroids (Si+Gr)	14440	0.1	12
		0.2	12
		0.3	12
		0.2	6
		0.2	8
Spheroids (Si+Gr)	25896	0.1	12
		0.2	12
		0.3	12
Spheroids (Si+Gr)	1184	0.2	6
Spheroids (Si+Gr)	152	0.2	4

V_{solid} is the solid material inside the grain and V_{total} is the total volume of the grain (Hage and Greenberg, 1990a,b). Accordingly, the porosity p for the composite grains varies between $0 < p < 1$ (for more details on porosity and porous grains see Vaidya and Gupta, 1997, 1999). Using the modified code for the composite grains, we have studied composite grain models with a host sphere (or spheroid) containing $N = 57856$, 14440 and 25896 dipoles each carved out from $48 \times 48 \times 48$, $48 \times 24 \times 24$ and $48 \times 32 \times 32$ dipole sites respectively. The composite grain models with $N = 1184$ and 152 ($p = 60$ and 80%, respectively) are also generated and are used to study the effect of porosity on the scattering properties of the composite grains. The volume fractions of the graphite inclusions used are 10, 20 and 30%. The inclusion size is labeled by the number of dipoles n across the diameter of an inclusion (see Table 1) (Chylek et al., 2000). The equivalent volume radius for the inclusion is given by $r_{eq} = (3n/4\pi)^{1/3}d$. For more details on the computer code and the corresponding modification in the DDA code, see Dobbie (1999).

Figure 1a and b illustrate the composite grain model for a typical spheroid ($N = 14440$), used in the present study. Figure 1a shows the host spheroid (sites are shown in green color circles) with the embedded inclusions (shown in red color circles). Since all the embedded inclusions cannot be seen and only the ones at the outer periphery are visible (Figure 1a), in the Figure 1b we show the positions of all these inclusions in the host grain (best seen in the electronic version).

It is to be emphasized that in the composite grain model considered in the present study, the inclusions are embedded in the host sphere, their positions are chosen randomly and they are not overlapping; whereas in the aggregate grain model (Xing and Hanner, 1997) of monomers, one monomer in the center is surrounded by the rest of the monomers; which are either overlapping, touching or separated.

The optical constants for silicate and graphite ($m = 1.71 + 0.033i$ and $4.04 + 2.58i$, respectively) at wavelength of 2.2 μm, used in the present calculations are obtained from Draine (1985). Table 1 shows the parameters for the composite grain models considered in the present study. Here Si+Gr denotes the composite grain having silicate as the material for the host sphere or spheroid and graphite as the material for the inclusion.

We have used the size range a_{eq} from 0.05 to 1.0μ, which corresponds to equivalent volume size parameter $X = 2\pi a_{eq}/\lambda$ from 0.14 to 3.0 at the wavelength of 2.2 μm, where a_{eq} is the radius of the sphere of equivalent volume of the host grain. For all the grain models and grain sizes considered in the present study, the DDA criterion $|m|kd \leq 1$ is satisfied.

To model the randomly oriented grains it is necessary to get the scattering properties of the composite grains averaged over all of the possible orientations; i.e. $\beta(0 \to 360°)$, $\theta(0 \to 180°)$ and $\phi(0 \to 360°)$; (see Draine

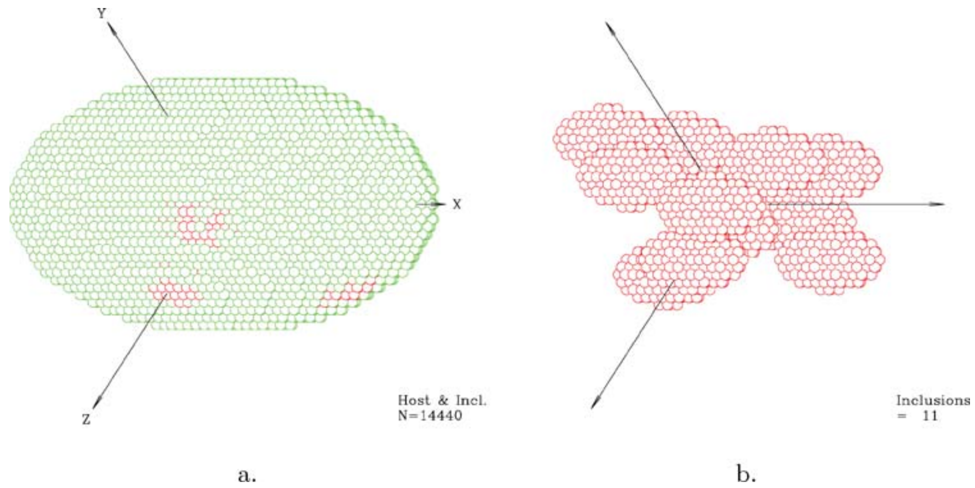

Fig. 1 A typical non-spherical composite grain with a total of $N = 14440$ dipoles. (a) Shows the inclusions embedded in the host spheroid such that only the ones placed at outer periphery are seen and (b) shows the inclusions

and Flatau, 1998). In the present study we use three values for each of the orientation parameters (β, θ, ϕ) i.e. averaging over 27 orientations; which we find quite adequate; higher number of orientations (e.g. Xing and Hanner, 1997; Yanamandra-Fisher and Hanner, 1999) would require considerable computer cpu time. It should be noted that we have also used grain size distributions for averaging and folding up the curves at 0° and 180° scattering angle (see for example Jockers, 1997).

3. Results and discussion

To be consistent with the comet dust composition, i.e. silicate and absorbing material with high carbon content (Kissel et al., 1986), we have selected silicate and graphite as the constituent materials for the composite grains in the present study. Earlier, Vanysek and Wickramasinghe (1975) had also suggested silicate and graphite particles as possible constituents in the cometary material. A two component grain model with 'rough' grains was also suggested by Lamy et al. (1987) and Brooke et al. (1987) to fit the observed polarization in the dust coma of comet Halley. In this paper we have made a systematic study of the effect of variation in the volume fraction and the size of the inclusions on the scattering properties of the composite grains. The composite grain models considered in the present study are shown in Table 1.

We have considered spherical and non-spherical composite grains in the size parameter range X from 0.14 to 3.0, corresponding to the radius a_{eq} of 0.05 to 1.0μ of the host grain at the wavelength of 2.2 μm.

3.1. Spheres

Figure 2(a–f) show the angular scattered intensity (i.e. S11) and the linear polarization P (i.e. $-$S12/S11) (Bohren and Huffman, 1983) for the composite grains with the host silicate sphere, containing $N = 57856$ dipoles and for three volume fractions (viz. 10, 20 and 30%) of graphite inclusions for a constant inclusion size ($n = 12$, i.e. $r_{eq} \sim 1.45$ d).

It is seen that the scattered intensity S11 for small composite grains ($X \sim 0.3$), is increasing with the volume fraction of the inclusions. For larger grains, i.e. $X \sim 1.5$ and 3.0 the scattered intensity S11 decreases with the increase in the volume fraction of the inclusions up to 90 and 50° scattering angles respectively, beyond these angles there does not seem to be any variation with the volume fractions. It should be noted that these large grains ($X \sim 1.5$ and 3.0) do not show any back scattered enhancement. Figure 2b shows the linear polarization for small ($X \sim 0.3$) grains. The polarization is maximum around 90° but there is no variation with the volume fraction. For the grains with $X \sim 1.5$, polarization P, shows considerable variation with the volume fraction of the inclusions (Figure 2d). It is seen that the angle of maximum polarization shifts from about 125° for the volume fraction $f = 0.1$ to 90° for fraction $f = 0.2$ and to 70° for the volume fraction $f = 0.3$ of the inclusions. The degree of polarization P also decreases from about 0.6 to 0.2 as the volume fraction of the graphite inclusion increases. For large grains,

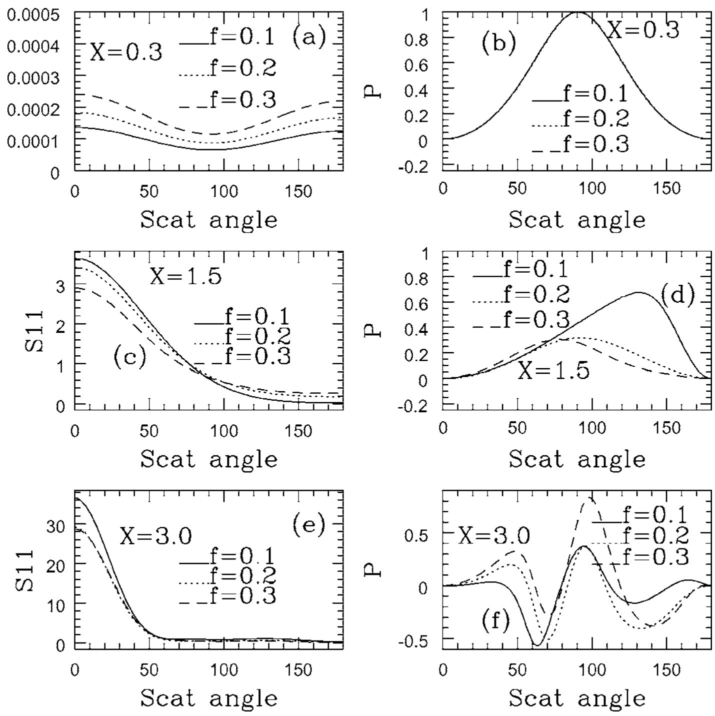

Fig. 2 Scattered intensity (S11) and polarization P for the spherical composite grain ($N = 57856$), with silicate as host sphere and graphite inclusions showing variations with various volume fractions

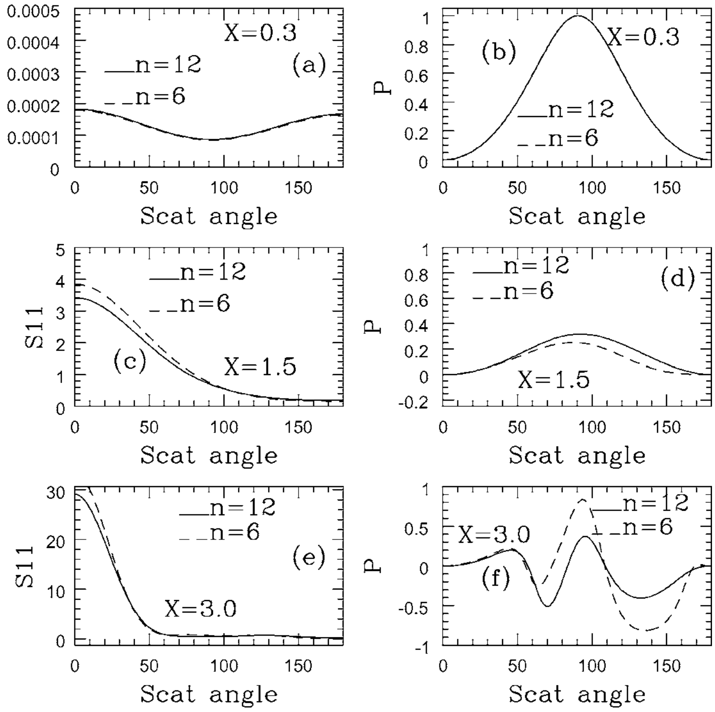

Fig. 3 Scattered intensity (S11) and polarization P for the Spherical Composite grain ($N = 57856$), with silicate as host sphere and graphite inclusions showing variations with various inclusion sizes for a fixed volume fraction of 20%

$X = 3.0$, these curves show negative polarization for all the volume fractions of inclusions and the positive polarization increases with the volume fraction f of the graphite inclusions. Figure 3(a–f) show the scattering function for spherical composite grain for two inclusion sizes (viz. $n = 6$ and 12) at a constant volume fraction of the inclusion ($f = 0.2$). It is seen that there is no appreciable variation in the scattered intensity S11 with the inclusion size. The scattered intensity is flat beyond 90°, i.e. there is no back scattering. The degree of polarization P for grains upto ($X = 1.5$) does not show appreciable variation with the inclusion size. For larger grains ($X = 3.0$) P is higher for large inclusion size (i.e. $n = 12$) than that is obtained for $n = 6$. However, there is no shift in the position of the maximum polarization $P_{\max}$, i.e. the angle of maximum polarization, with the inclusion size.

We have also compared the results on the composite grains using DDA with the results obtained using the Maxwell Garnett effective medium approximation (EMA) (Bohren and Huffman, 1983). Using EMA we have obtained the optical constants for the composite grains and have used these constants in conjunction with Mie theory to calculate the scattered intensity and the polarization P. The EMA results for the composite Si+Gr (i.e. silicate host and graphite as inclusions) grain models deviate considerably from DDA results (Figure 4a–f). EMA results do not agree with DDA results for Si+Gr grain models because the EMA does not take into account the inhomogeneities within the grain, i.e. internal structure, voids, surface roughness etc. (see e.g. Perrin and Lamy, 1990; Wolff et al., 1994, 1998). Since Maxwell–Garnet mixing rules provide the extreme cases of the possible values of the effective dielectric constants of a two component mixture (Chylek et al., 2000) we have used the Maxwell–Garnet mixing method. Investigating the effects of compositional inhomogeneities and fractal dimension on the optical properties of astrophysical dust Bazell and Dwek (1990) have found Maxwell–Garnett mixing rule better than the Bruggeman rule (Bohren and Huffman, 1983). However, the criteria of validity of respective theories are not clear (Bohren and Huffman, 1983; Perrin and Sivan, 1990). It would be therefore very useful and advantageous to compare the DDA results for the composite grains (with varying inclusion sizes and volume fractions) with those obtained by other EMA/Mie type series solution techniques in order to examine the applicability of several mixing rules (see e.g. Chylek et al., 2000; Wolff et al., 1998).

3.2. Spheroids

The main purpose of the present study is to use the results of the composite grains to interpret the observed scattering properties of the cometary dust. Several studies have shown that the cometary dust particles are nonspherical (see for example Greenberg, 1980; Jockers, 1997). The collected interplanetary dust particles (IDPs) of likely cometary origin are nonspherical (Brownlee, 1978). Vaidya and Desai (1996) and Kiselev and Velichko (1998) have also suggested nonspherical porous particles to explain the scattering properties of cometary dust. Also, spherical particles show resonances in the scattered intensity and polarization (Bohren and Huffman, 1983) which are not present in the nonspherical

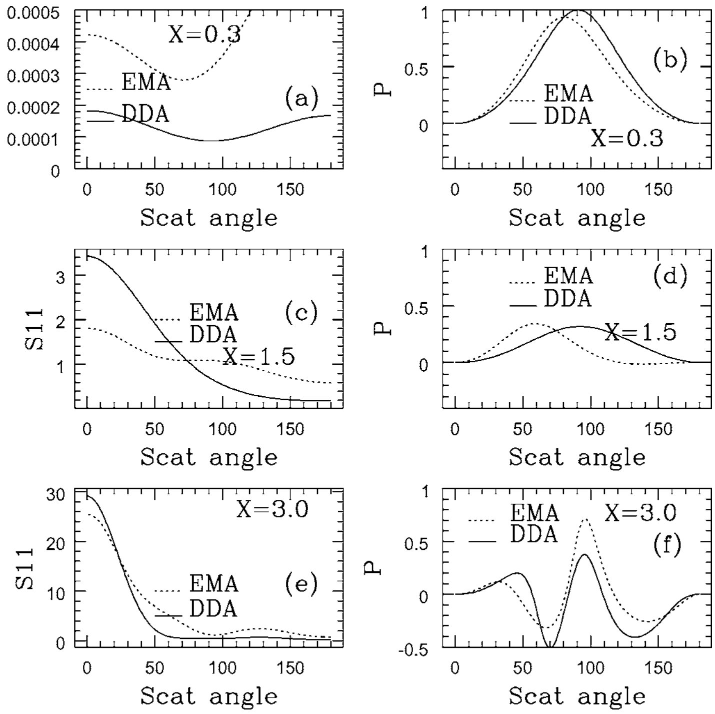

Fig. 4 Comparison of scattered intensity (S11) and Polarization P for the DDA Spherical Composite grain ($N = 57856$), Si+Gr, and EMA for various grain size parameters X

particles and are not observed in cometary dust. Hence, in addition to the spherical grains, we have also studied the scattering-properties for the composite spheroidal grains.

Figure 5(a–f) show the scattered intensity and the polarization P for the composite grains containing a host spheroid with 14440 dipoles for three volume fractions of the inclusions. It is seen that for these spheroidal composite grains there is no appreciable variation in the scattered intensity S11 with the volume fraction of the inclusions. The scattered intensity curves do not display any back scattering. The linear polarization P for small ($X \sim 0.3$) spheroidal composite grains peaks around 90° and there is no variation with the volume fractions of inclusions. For grains with $X = 1.5$, the angle of maximum polarization shifts with the variation in the volume fraction of inclusions i.e. it shifts from 120° for $f = 0.1$ to 80° for $f = 0.3$. Figure 5f shows linear polarization for large grains $X = 3.0$ for three volume fractions. It is seen that the composite grain with a fraction of $f = 0.1$ and 0.2 produce negative polarization but with $f = 0.3$ of graphite inclusion, the negative polarization vanishes.

We have also calculated the scattered intensity for the spheroidal composite grains ($N = 14440$) for three inclusion sizes, viz. $n = 6$, 8 and 12, at a constant volume fraction of 20%. The scattered intensity does not show variation with the inclusion size (Figure 6a,c,e). The polarization P for small grains, $X = 0.3$ does not show any variation with the inclusion size. For the grains with $X = 1.5$, the angle of maximum polarization $P_{\max}$ shifts from about 120° for $n = 6$ to 90° for $n = 12$ (Figure 6d). For large grains i.e. $X = 3.0$ these three curves show negative polarization for both these inclusion sizes viz. $n = 6$ and 12 (Figure 6f).

Figure 7(a–f) show 3-D plots of scattered intensity S11 and linear polarization P, for the composite grains with $N = 14440$ and 152 and grain sizes $a_{\rm eq} = 0.1$–1.0μ with $f = 0.2$. It is seen that for the composite grains $N = 14440$, S11 curves are fairly flat for all the grain sizes; however, for the composite grains with $N = 152$ and for the grain sizes $a_{\rm eq} > 0.5\mu$, the S11 curves show backscattering, i.e. these curves show enhancement in the backward direction. The linear polarization P for the composite grains sizes $a_{\rm eq} = 0.1$–0.5μ increases with the scattering angle, it becomes maximum around 90° and goes to zero at 180°. The curves for larger grain sizes (i.e. $a_{\rm eq} > 0.5\mu$) show negative polarization at intermediate scattering angles before they fold-up to $P = 0$ at 180° (Figure 7b and d). It is to be noted here that the composite grains with $N = 152$ are porous with porosity $p = 80\%$, (p is defined in Section 2). These results show that the composite grains with high porosity can produce backscattering,which is observed in cometary dust (Hage and Greenberg, 1990b). Petrova et al. (2000) have on the other hand shown that more compact particles display the negative polarization and the backscattered intensity better than as compared to porous particles.

In order to interpret the observed angular scattering and linear polarization in cometary dust, we have used a power law size distribution for the composite grains.

Figure 8(a–f) show the scattered intensity S11 and linear polarization P for the composite grains with $N = 14440$,

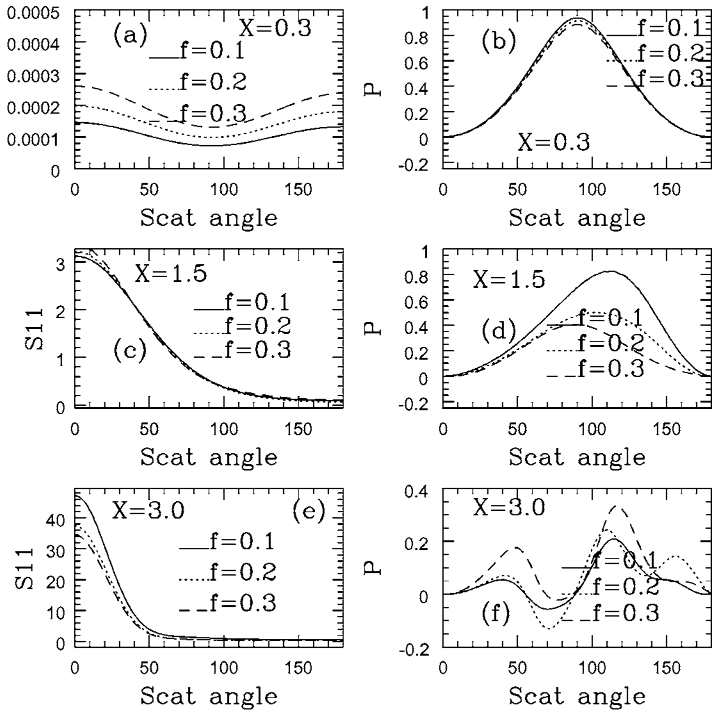

Fig. 5 Scattered intensity (S11) and polarization P for the non-spherical composite grain ($N = 14440$), with silicate as host sphere and graphite inclusions showing variations with various volume fractions

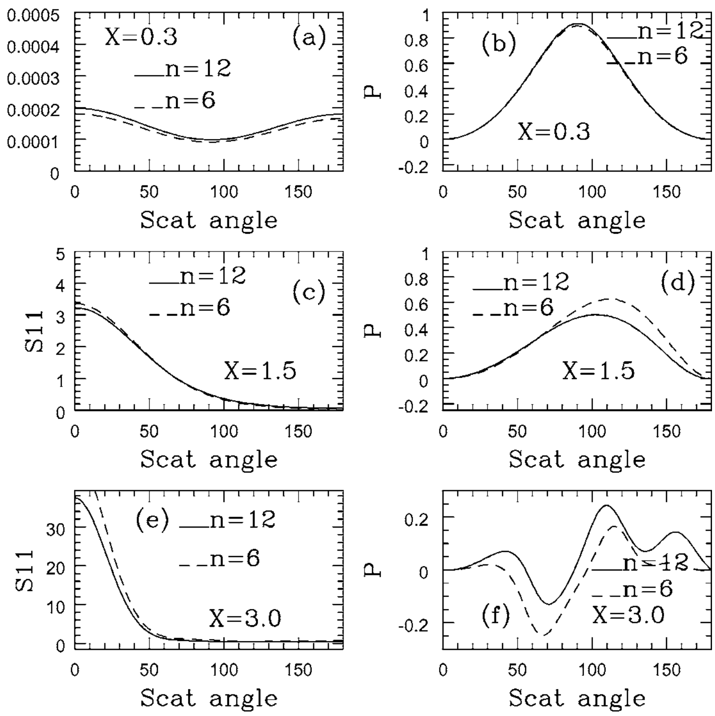

Fig. 6 Scattered intensity (S11) and polarization P for the non-spherical composite grain ($N = 14440$), with silicate as host sphere and graphite inclusions showing variations with various inclusion sizes for a fixed volume fraction of 20%

1184 and 152 for a size distribution, $n(a)da \propto X^{-q}$, with the index $q = 3.5$ in the size parameter range of $X = 0.25$–2.5 (i.e. $a_{\rm eq} = 0.1$–1.0μ). It is seen from Figure 8a and b that the spheroidal grains with $N = 14440$ and 1184 and grain size distribution of $a_{\rm eq} = 0.1$–1.0μ do not show back scattering. Figure 8(c) shows the scattered intensity for spheroidal composite grains with $N = 152$, i.e. with 80% porosity which clearly shows the back scattering. Linear polarization curves for $N = 14440$ and 1184 in Figure 8(d and e) do not show maxima and they are fairly flat, i.e. they are showing almost constant degree of polarization over a wide range of scattering angles. However, the linear polarization curves for spheroidal grains with $N = 152$ (Figure 8f) shows maximum degree of polarization at 90°.

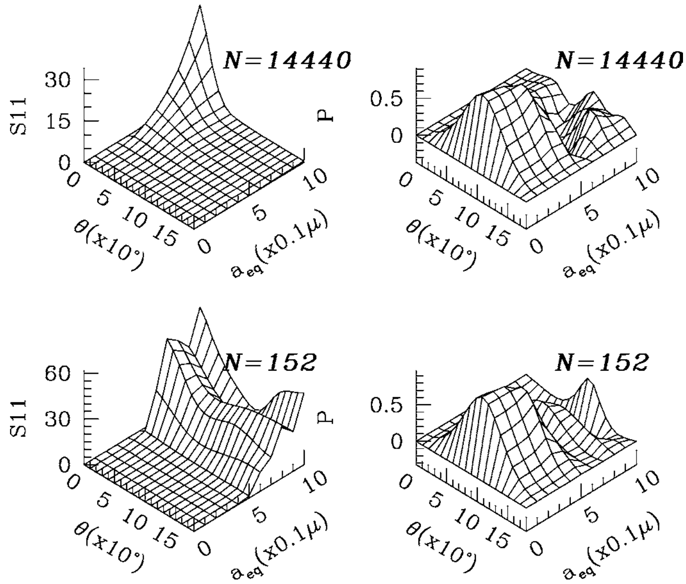

Fig. 7 3D plots of scattering intensity S11 and linear polarization (P) for composite spheroidal grains with silicate host spheroid and 20% graphite inclusions. The vertical axes are for S11 and degree of linear polarization P; the axes marked as 0 denotes the scattering angle ($\times 10^{\circ}$) in the range 0–180° and the third axis is for grain size $a_{\mathrm{eq}} = 0.1$–1.0μ

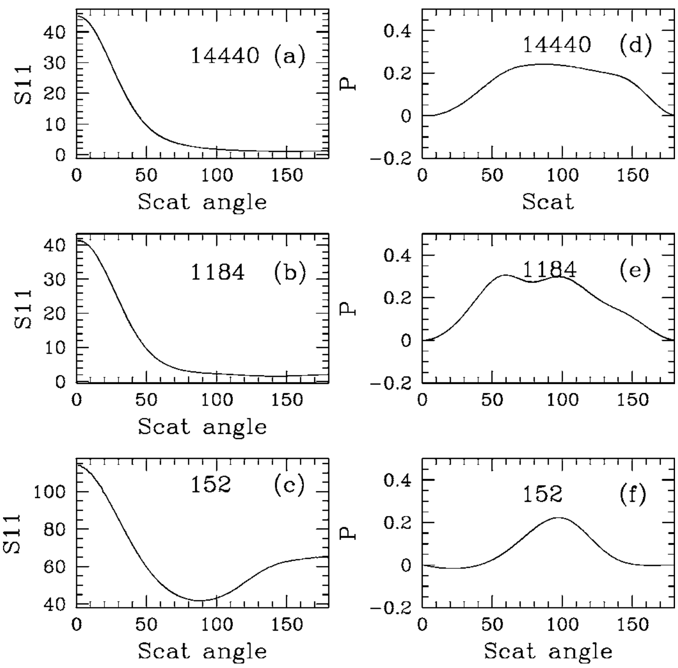

Fig. 8 Scattered intensity S11 and linear polarization P for the composite grain size distribution $X = 0.28$–2.8 ($a_{\mathrm{eq}} = 0.1$–1.0μ), $f = 0.2$

Figure 9(a–f) show S11 and P for smaller grain size distribution, i.e. $a_{\mathrm{eq}} = 0.06$–0.6μ. For this small size distribution also, the spheroidal composite grains with $N = 14440$ and 1184 do not show back scattering (see Figure 9a and b), whereas the spheroidal grain with $N = 152$ (i.e. with ~80% porosity) does show the back scattering (Figure 9c). Linear polarization curves for all the three grain models show a maxima at scattering of 90° (Figure 9d–f).

Figure 10(a–d) show the linear polarization for the spheroidal composite grains with $N = 14440$ and $N = 25896$ for a distribution of grain sizes with three volume fractions. Figure 10a shows polarization for spheroidal composite grains ($N = 14440$) for three volume fractions with a power law size distribution, in the size parameter range of $X = 0.17$–1.7, i.e. $a_{\mathrm{eq}} = 0.06$–0.6μ. It is seen that for all three fractions linear polarization P increases with scattering angle, reaches maximum around 90° and fold-up to zero at 180°. It is also seen that P decreases with the volume fraction of the inclusions at the angle of maximum polarization for this size distribution. In Figure 10b, P increases with volume fraction f for the larger size distribution (i.e. $a_{\mathrm{eq}} = 0.1$–1.0μ. In Figure 10c and 10d, we show linear polarization curves for the smaller and larger size distribution of spheroidal grains for $N = 25896$.

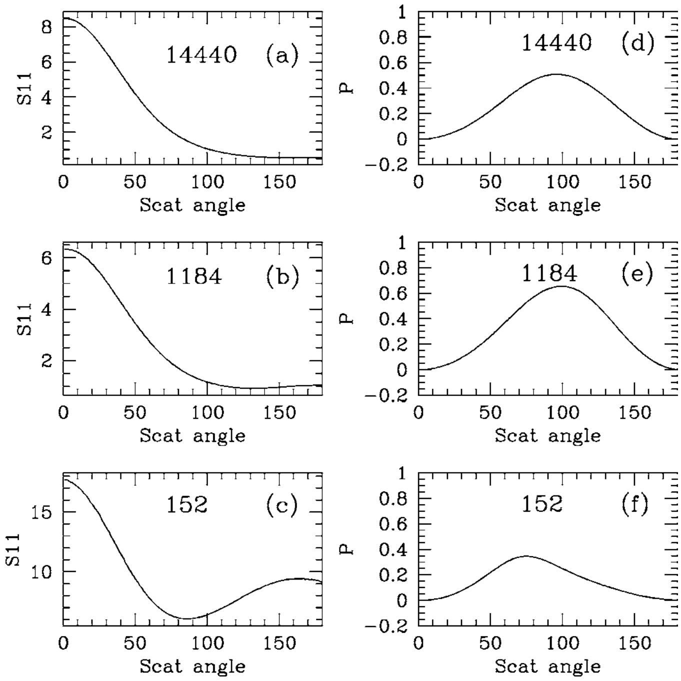

Fig. 9 Scattered intensity S11 and linear polarization P for the composite grain size distribution $X = 0.17–1.7$ ($a_{\text{eq}} = 0.06–0.6\mu$), $f = 0.2$

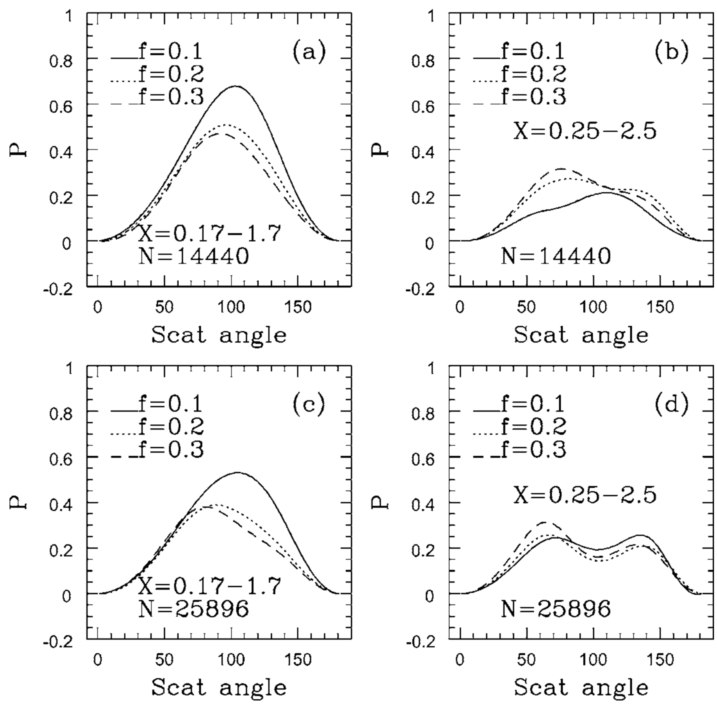

Fig. 10 Linear polarization P for spheroidal composite grains with size distributions $a_{\text{eq}} = 0.06–0.6\mu$, and $a_{\text{eq}} = 0.09–0.9\mu$

These results on the spheroidal (Si+Gr) composite grain models with volume fraction of inclusions *f* between 0.1 and 0.3, at infrared wavelength of 2.2 μm show maximum positive polarization of about 0.3 around 90° and becomes zero at 180°. These results seem to be consistent with the linear polarization observed in most of the cometary dust (see for example Kelley et al., 2004). However, it is to be noted these composite grain models do not show negative branch of polarization at large scattering angles ∼140–150°, observed in some comets.

Figure 11 shows linear polarization for composite grains with $N = 25896$, 14440 and 152 alongwith with the observed polarization curves of Comet Halley at 2.2μm (Brooke et al., 1987 represented with filled squares) and for observed data of comets given by Kelley et al. (2004) represented with open squares. It should be noted that these models with a very

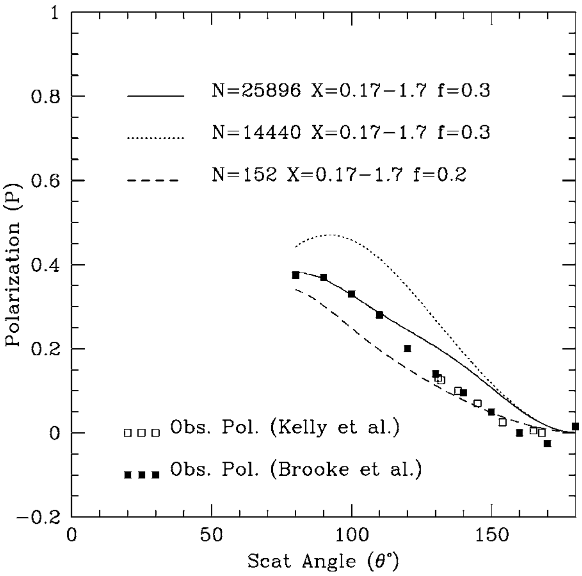

Fig. 11 Linear polarization P for composite grain models alongwith the observed linear polarization data for comets

specific size distribution of composite grains and volume fractions are not unique.

These results on the composite grains indicate that a very specific grain size distribution is required for a good fit to the observed scattering and polarization curves in comets. Recently Petrova et al. (2000) have also studied the scattering properties of aggregate silicates and they have also found that the shape of the polarization curve is very sensitive to the size and size distribution of the grains. Kerola and Larson (2001) have used T-matrix method to calculate the polarization upto the scattering angle 160° for prolate spheroidal crystalline olivine particles. Their results are compared well with the comets' measured polarization at the wavelengths 0.4845 and 0.684 μm.

4. Summary and conclusions

The scattering properties, i.e. the angular scattered intensity and the linear polarization for the composite grains with the silicate and graphite as the constituent materials are studied with various inclusion sizes and volume fractions. We have studied these properties for spherical and spheroidal composite grains. We have also compared the results on the composite grains obtained using DDA with those obtained using EMA. Our main conclusions are as follows:

1. For small ($X \sim 0.3$) spherical composite (Si+Gr) grains, the scattered intensity (S11) is found to be increasing with the volume fraction of the inclusions. For larger grains ($X \geq 1.5$), S11 is found to be decreasing with the volume fraction of the inclusions. However, the back scattering or the scattering enhancement in the back direction is not seen for these spherical composite grains.
2. For small spherical grains ($X \sim 0.3$) the linear polarization does not seem to vary with the volume fraction of the inclusion. For sizes $X \geq 1.5$, $P_{\max}$ shifts with the volume fraction of the inclusions.
3. The EMA results for the composite grains (Si+Gr) deviate considerably from the DDA results.
4. Spheroidal composite grains with silicate as the host material and inclusions of graphite with volume fractions of $f = 0.2$ and 0.3 show the maximum positive polarization of about 0.3 around 90°. The polar ization curves we have obtained for the spheroidal composite grains with axial ratios ∼1.3–2.0 in the size parameter range $X = 0.17$–1.7, containing silicate as the host material with the inclusions of highly absorbing materials such as graphite, resembles the observed polarization curve in comets (Brooke et al., 1987; Kiselev and Velichko, 1998; Kelly et al., 2004). However, these composite grain models do not produce negative polarization at large scattering angles (i.e. >150°), observed in some comets in near infra-red (NIR) wavelength region. It is to be noted that the so called negative branch of polarization is not observed in all the comets at 2.2 μm (see e.g. Kelly et al., 2004).

The composite grain models with very high porosity, about 80%, show back scattered enhancement observed in comets. Highly porous grains with about 90% porosity have also been suggested by Hage and Greenberg (1990b) to produce the observed backscattered intensity.

Our results on the composite grains with silicate as the host material and graphite inclusions show that a very specific volume fraction of inclusion and a very specific grain size distribution may be required to explain all the observed properties in cometary dust. Yanamandra-Fisher and Hanner (1999) have suggested a broader grain size distribution to explain all the observed scattering properties in cometary dust. It would also be interesting to study the scattering properties of the composite particles at few more wavelengths which would help to explain the polarization color effect (i.e. higher polarization in red than in green) found in several comets (see e.g. Levasseur-Regourd et al., 1996). Laboratory scattering measurements on the composite grains at microwave wavelengths (e.g. Gustafson and Kolokolova, 1999) would also help towards better interpretation of the observed scattering from cometary dust.

Acknowledgements We thank Bruce Draine and Piotr Flatau for providing the DDSCAT code. DBV thanks IUCAA for continued support towards this research. This work on composite grains was initiated during DBV's visits to Dalhousie University, Halifax, Canada in years 1999 and 2000.

References

Bazell and Dwek, E.: ApJ **360**, 142 (1990)
Bohren, C.F., Huffman, D.R.: in Absorption and Scattering of Light by Small Particles, Wiley, New York, p. 217 (1983)
Bradley, J.P., Humecki, H.J., Germany, M.S.: ApJ **394**, 643 (1992)
Brooke, T.Y., Knacke, R.F., Joyce, R.R.: A&A **187**, 621 (1987)
Brownlee, D.: in Cosmic Dust, McDonnell, J.A.M. (ed.), Wiley, New York, p. 295 (1978)
Brownlee, D.: in Interstellar Processes, Hollenbach, D.J., Thompson, H. (eds.), Reidel, Dordrecht Heidelberg, p. 513 (1987)
Chylek, P., Srivastava, V., Pinnick, R.G., Wang, R.T.: Appl. Opt. **27**, 2396 (1988)
Chylek, P., Videen, G., Geldart, D.J.W., Dobbie, J., William, H.C.: in Light Scattering by Nonspherical Particles, Mishchenko, M., Hovenier, J.W., Travis, L.D. (eds.), Academic Press, New York, p. 274 (2000)
Dobbie, J.S.: Radiative Characteristics of Aerosols and Clouds. PhD Thesis, Dalhousie University, Canada (1999)
Draine, B.T.: ApJS **57**, 587 (1985)
Draine, B.T.: ApJ **333**, 848 (1988)
Draine, B.T., Flatau, P.J.: J. Opt. Soc. Am. **11**, 1491 (1994)
Draine, B.T., Flatau, P.J.: User notes on DDA code version ‘ddscat5a9’ (1998)
Draine, B.T., Goodman, J.J.: ApJ **405**, 685 (1993)
Greenberg, J.M.: in Focusing in on Particle Shape in Light Scattering by Irregularly Shaped Particles, Schuerman, D.W. (ed.), Plenum Press, New York (1980)
Gustafson, B.A.S., Kolokolova, L.: J. Geophys. Res. **104**(D24), 31711 (1999)
Hage, J.I., Greenberg, J.M.: in Origin and Evolution of Interplanetary Dust, Levasseur-Regourd, A.C., Hasegawa, H. (eds.), Kluwer Academic, Japan, p. 261 (1990a)
Hage, J.I., Greenberg, J.M.: ApJ **361**, 251 (1990b)
Hanner, M.S.: in Electromagnetic and Light Scattering by Non-Spherical Particles, Gustaffson, B., Kolokolova, L., Videen, G. (eds.), Army Research Laboratory, Maryland, USA, p. 99 (2002).
Harker, D.E., Wooden, D.H., Woodword, C.E., Lisse, C.M.: ApJ **580**, 579 (2002)
Jessberger, E.K., Christofordis, A., Kissel, K.J.: Nature **332**, 691 (1988)
Jessberger, E.K.: Space Sci. Rev. **90**, 91 (1999)
Jockers, K.: Earth Moon Planets **79**, 221 (1997)
Jones, T.J., Gehrz, R.D.: Icarus **143**, 338 (2000)
Kelley, M.S., Woodward, C.E., Jones, T.J.: AJ **127**, 2398 (2004)
Kerola, D.X., Larson, S.M.: Icarus **149**, 351 (2001)
Kissel, J., 19 colleagues: Nature **321**, 280 (1986)
Kiselev, N.N., Velichko, F.P.: Icarus **133**, 286 (1998)
Lamy, P.L., Grun, E., Perrin, J.M.: A&A **187**, 767 (1987)
Levasseur-Regourd, A.C., Hadamick, E., Renard, J.B.: A&A **313**, 327 (1996)
Lumme, K., Rahola, J., Hovenier, J.W.: Icarus **126**, 455 (1997)
Perrin, J.M., Lamy, P.L.: ApJ **364**, 146 (1990)
Perrin, J.M., Sivan, J.P.: A&A **228**, 238 (1990)
Petrova, E.V., Jockers, K., Kiselev, N.N.: Icarus **148**, 526 (2000)
Purcell, E.M., Pennypacker, C.R.: ApJ **186**, 705 (1973)
Vanysek, V., Wickramasinghe, N.C.: Ap&SS **33**, L19 (1975)
Vaidya, D.B., Desai, J.N.: in Physics, Chemistry and Dynamics of Interplanetary Dust, Gustafson, B.A.S., Hanner, M.S. (eds.), APS conf. series **104**, p. 433 (1996)
Vaidya, D.B., Gupta, R.: A&A **328**, 634 (1997)
Vaidya, D.B., Gupta, R.: A&A **348**, 594 (1999)
Vaidya, D.B., Gupta, R., Dobbie, J.S., Chylek, P.: A&A **375**, 584 (2001)
Wolff, M.J., Clayton, G.C., Martin, P.G., Sculte-Ladlback, R.E.: ApJ **423**, 412 (1994)
Wolff, M.J., Clayton, G.C., Gibson, S.J.: 1998, ApJ **503**, 815
Xing, Z., Hanner, M.S.: 1997, A&A **324**, 805
Yanamandra-Fisher, P., Hanner, M.S.: 1999, Icarus **138**, 107